Chapter 19
Modeling, Simulation, and Experimental Analysis of Liquid Sloshing Dynamics

Johannes Schröck, Johannes Wenninger, Erwin Karer, and Andreas Eitzlmayr

Abstract For the simulation of liquid sloshing, particle simulation methods allow a detailed investigation of the acting dynamics. Since these methods usually go along with considerable computational loads the application of alternative, simplified models is a usual proceeding. However, the parameters of the simplified model can not be directly computed from physical quantities in the general case, such that parameter identification based on measurements is required. In applications where experimental investigation is expensive, the use of particle simulation results for parameter identification can be a promising alternative. This contribution considers the identification of the parameters of a simplified model for different container geometries and filling levels based on smoothed particle hydrodynamics (SPH) simulation results. The comparison with experimental data verifies the accuracy and sensitivity of both the used particle model as well as the simplified model.

19.1 Introduction

New mechatronic conveyor concepts like the long stator linear motor (LLM) actuator give additional degrees of freedom for the transportation of objects compared to conventional conveyor systems. The conveyed objects get moved by separate shuttles individually controlled based on their position along the LLM actuator. This provides completely new options for object transportation, processing, and throughput optimization. The transport speed can be adapted to the radius of curvature along the transport track. The motion of the objects can be synchronized to each individual processing cell along the track. The flow of objects can be efficiently split to different tracks and several flows are easily brought together to a common track. Using individual controllable transportation shuttles instead of a common conveyor belt may be a key-enabler component for agile production.

J. Schröck (✉) · J. Wenninger · E. Karer · A. Eitzlmayr
Linz Center of Mechatronics GmbH, Altenberger Straße 69, 4040 Linz, Austria
e-mail: johannes.schroeck@lcm.at

H. Irschik et al. (eds.), *Dynamics and Control of Advanced Structures and Machines*,
Advanced Structured Materials 156,
https://doi.org/10.1007/978-3-030-79325-8_19

A specific application is the fast transport of open containers filled with liquid. Depending on acceleration and track geometry, the dynamics can cause the liquid spilling over the container opening. Up to now, sloshing is prevented by a conservative setup of the transportation system. Using individually controlled transport shuttles instead of a common conveyor belt allows to accordingly adapt velocity profiles for the movement, which limit the sloshing angle to a predefined value. Hence, each segment of the track can be safely passed through by simultaneously maximizing the throughput. In order to determine the optimal shuttle trajectory along an arbitrary predefined track, a model-based approach is required. In this context, it is sufficient to consider the dominant sloshing characteristics.

The simplest model representing a sloshing liquid is a pendulum model with properly defined parameter values for the pendulum mass, pendulum length, and damping coefficient. For containers with circular or square cross sections at least mass and length parameters can be derived from analytical considerations of container geometry, filling level and liquid density, see, e.g., [1]. In the general case, where a more complex container geometry is used, the correct parameters have to be determined by parameter identification methods based on measurements from experimental investigations. Clearly, experimental investigations are often expensive and time-consuming. Therefore, this paper proposes to use SPH simulation results for identification of the parameters of the pendulum model. As a first step for a general approach, this procedure is validated by considering a simple container geometry. The comparison with measurements from experimental investigations illustrates the reliability of this approach.

The paper is structured as followed: Sect. 19.2 describes the experimental test-bed. Section 19.3 presents the mathematical model of the considered pendulum model. Identification and validation of the model parameters is reported in Sect. 19.4 based on measurement results. Section 19.5 shows the simulation results based on SPH, which are used for parameter identification of the pendulum model in Sect. 19.6.

19.2 Experimental Test-Bed

The test-bed consists of two linear axes with ball screw drives from *HIWIN* (HM060S and HM040S) which enable a range of motion of 0.5×0.3 m in the (x, y)-plane, see Fig. 19.1. Each linear axis is driven by a *B&R* synchronous motor of the 8LS series, that is controlled by an *ACOPOS* servo drive (8V1010). The control task is implemented on a *B&R Power Panel* C70 PLC with a cycle time of 2 ms using PID position control. The liquid container to be transported is mounted to the y-axis via a high accuracy 3-axis-force sensor (K3D60a) from *ME-Messsysteme GmbH* with nominal measuring force of ± 50 N and accuracy class 0.05%. *DEWETRON* DAQP-STG measurement amplifiers are used to connect the force signals to the PLC via an analog input X20 module. The measurement accuracy of the container position results from the motor encoder (10^4 increments per revolution) and the ball screw pitch of 10 mm. Data acquisition of force, position and velocity is realized by means of the PLC with a sample time of 2 ms.

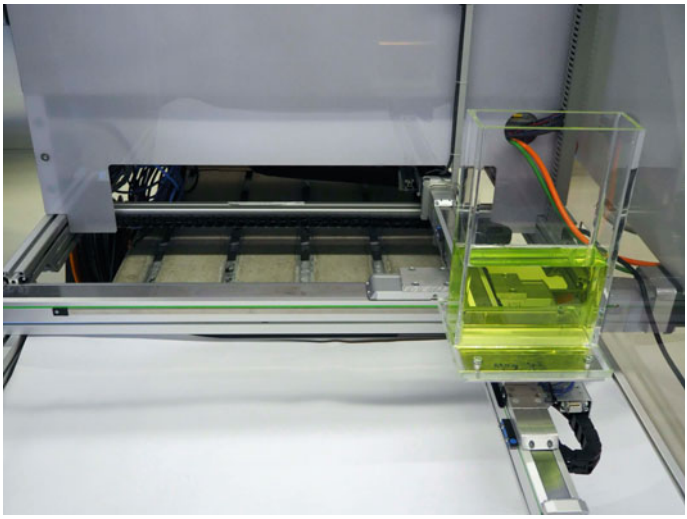

Fig. 19.1 Testbed with liquid filled container mounted on two linear axes

The test-bed is used to move containers filled with different amounts of water along certain trajectories in order to investigate the dynamics of the sloshing water by means of the force measurements. It will be shown, that the behavior of the liquid can be accurately reproduced by means of both proper defined particle simulations and a simplified model, suitable for real-time simulations and model-based control applications.

19.3 Simple Model for Sloshing

In this contribution, the focused application of transporting liquid-filled container results in a smooth sloshing behavior, i.e., there appears no splashing and no separation of the liquid volume in different entities. The container is considered to be open at the top, and a continuous free liquid surface is assumed. In this case, linear sloshing can be supposed, which means the sloshing can be represented by its natural frequencies [1]. Since the main contribution concerning sloshing forces and sloshing angle corresponds to the first sloshing mode, the pendulum model is a satisfactory choice.

In the following investigations, it turns out that only a certain amount of the liquid mass contributes to the sloshing dynamics. For this reason, the liquid mass M_{liq} is separated into two parts, $M_{liq} = M_{liq,r} + m$, with m responsible for the sloshing and $M_{liq,r}$ representing the remaining liquid mass. Hence, the pendulum model can be defined by the two masses M and m and the pendulum length l as shown in the scheme in Fig. 19.2a with $M = M_{liq,r} + M_t = M_{liq} - m + M_t$, where

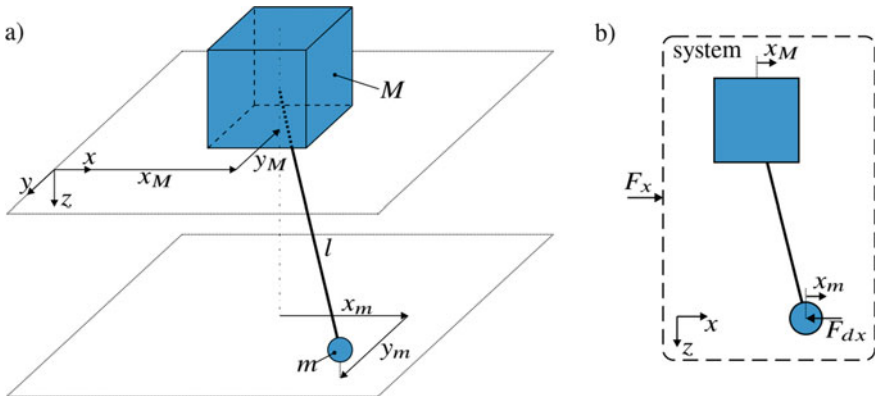

Fig. 19.2 Scheme of the pendulum model (**a**) and linear momentum in x-direction (**b**)

M_t represents the mass of the empty container. The masses have two degree of freedom $\{x_M(t), y_M(t)\}$ and $\{x_m(t), y_m(t)\}$. The governing equations of motion can be derived by means of the Euler-Lagrange approach, i.e.,

$$\frac{d}{dt}\left(\frac{\partial T}{\partial \dot{\mathbf{q}}}\right)^T - \left(\frac{\partial T}{\partial \mathbf{q}}\right)^T + \left(\frac{\partial V}{\partial \mathbf{q}}\right)^T = \mathbf{Q}, \tag{19.1}$$

where $\mathbf{q}(t) = [x_m(t), y_m(t)]^T$ represents the generalized coordinates $T = \frac{1}{2} m \mathbf{v}_m^T \mathbf{v}$ the kinetic, and $V = -m\mathbf{g}^T \mathbf{r}_m$ the potential energy with the displacement vector $\mathbf{r}_m(t)$ and the velocity vector $\mathbf{v}_m(t)$ of the point mass m given by

$$\mathbf{r}_m(t) = \begin{bmatrix} x_M(t) + x_m(t) \\ y_M(t) + y_m(t) \\ \sqrt{l^2 - x_m(t)^2 - y_m(t)^2} \end{bmatrix}, \mathbf{v}_m(t) = \begin{bmatrix} \dot{x}_M(t) + \dot{x}_m(t) \\ \dot{y}_M(t) + \dot{y}_m(t) \\ \dfrac{-x_m(t)\dot{x}_m(t) - y_m(t)\dot{y}_m(t)}{\sqrt{l^2 - x_m(t)^2 - y_m(t)^2}} \end{bmatrix}. \tag{19.2}$$

The generalized forces $\mathbf{Q}(t)$ result from additionally introduced viscous damping

$$\mathbf{Q}(t) = \left(\frac{\partial\, \mathbf{r}_m(t)}{\partial \mathbf{q}}\right)^T \mathbf{F}_r(t), \quad \mathbf{F}_r(t) = \begin{bmatrix} -d_{px}\, \dot{x}_m(t) \\ -d_{py}\, \dot{y}_m(t) \\ 0 \end{bmatrix}, \tag{19.3}$$

with $\mathbf{F}_r(t)$ being the damping forces based on individual damping parameters d_{px} and d_{py} in x- and y-direction. Finally, the governing equations of motion can be given in the form

$$\mathbf{M}\,\ddot{\mathbf{q}}(t) + \mathbf{G}(\mathbf{q}, \mathbf{u}, t) = \mathbf{Q}(t), \tag{19.4}$$

with the mass matrix $\mathbf{M}$, the vector of non-linear terms $\mathbf{G}(\mathbf{q}, \mathbf{u}, t)$, and the acceleration of the mass M as the inputs $\mathbf{u}(t) = [\ddot{x}_M(t), \ddot{y}_M(t)]^T$. For the parameter identification and validation of the model, the forces experienced by the high accuracy 3-axis-force sensor have to be considered. These forces are given by

$$F_x = (m + M)\,\ddot{x}_M + m\,\ddot{x}_m + d_{px}\,\dot{x}_m, \tag{19.5}$$
$$F_y = (m + M)\,\ddot{y}_M + m\,\ddot{y}_m + d_{py}\,\dot{y}_m, \tag{19.6}$$

which can be derived based on the linear momentum in x- and y-direction also, see Fig. 19.2b.

19.4 Parameter Identification and Validation with Measurements

The test-bed described in Sect. 19.2 is used to execute experiments with two different container geometries (circular and square cross section) and each of them with two different filling levels of water (1 l and 0.33 l). Three different trajectories for the movements are used, two open trajectories similar to semicircles with different radii (Fig. 19.3a), and a closed eight-shaped trajectory (Fig. 19.3c). In the following, the trajectories are called semicircular-shaped and eight-shaped. The deviations from a precise semicircle as well as the initial variation of the eight-shaped trajectory result from the applied PID position controller. However, since we are focusing on the sloshing behavior and successive experiments with the same settings that provide precisely the same results, these deviations represent no restrictions for the following investigations.

The parameter identification for the pendulum model is done via minimization of the error between measured and simulated forces Eq. (19.5) by adopting the values of the parameter set $\{m, l, d_{px}, d_{py}\}$.[1] For that, measurements with an duration of $\Delta t = 10$ s from experiments based on the semicircular-shaped trajectory with radius 80 mm are used, see Fig. 19.3a solid lines. The resulting parameter values are given in Table 19.1, where they are compared to values from analytical models from the literature [1]. These analytical models consider the container geometry with circular and square cross section but do not include damping. The parameters m and l are in excellent correspondence for all four container configurations.

Figure 19.4 confirms that with these parameters a very accurate agreement between measurements and simulation results can be achieved for all configurations. In order to illustrate the effect of the sloshing, Fig. 19.5b compares the arising forces for the investigated configurations relative to a rigid mass movement along the same

[1] The corresponding optimization was performed by means of the open source software SyMSpace [2].

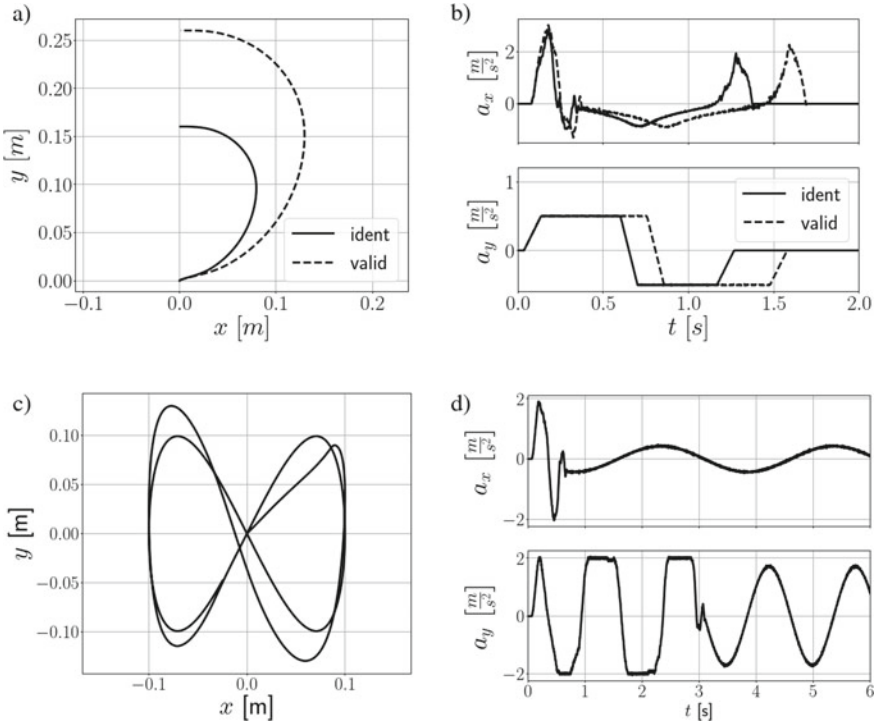

Fig. 19.3 Trajectories: **a** semicircular-shaped with radius $\in \{80, 130\}$mm and **c** eight-shaped; **b**, **d** corresponding acceleration signals $a_x(t)$ and $a_y(t)$ in x- and y-direction

trajectory, i.e., the sloshing forces are computed as the difference between measured forces and computed forces of a rigid mass. Obviously, there are minor differences in the evolution of the sloshing forces for square cross sections compared to circular cross sections. The amplitudes of the sloshing forces are not directly dependent on the filling level of the containers.

In order to validate the sensitivity of the identified parameter of the pendulum model, measurement and simulation results are compared for trajectories different from that used during the identification procedure. Figure 19.6a shows the evolution of the forces for a container with circular cross section and filling level 0.33 l moved along the semicircular-shaped trajectory with radius 130 mm, cf. Fig. 19.3a dashed lines. Obviously, this trajectory results in significantly lower sloshing compared the trajectory with radius 80 mm. Specifically, the sloshing represented by the force $F_y(t)$ is strongly reduced. While even for small amplitudes in $F_x(t)$ the agreement between measured and simulated results is highly accurate in Fig. 19.4, the deviations are higher with the trajectory of 130 mm. Nevertheless, the agreement between measured and simulated results is excellent, in particular during the motion of the liquid-filled container.

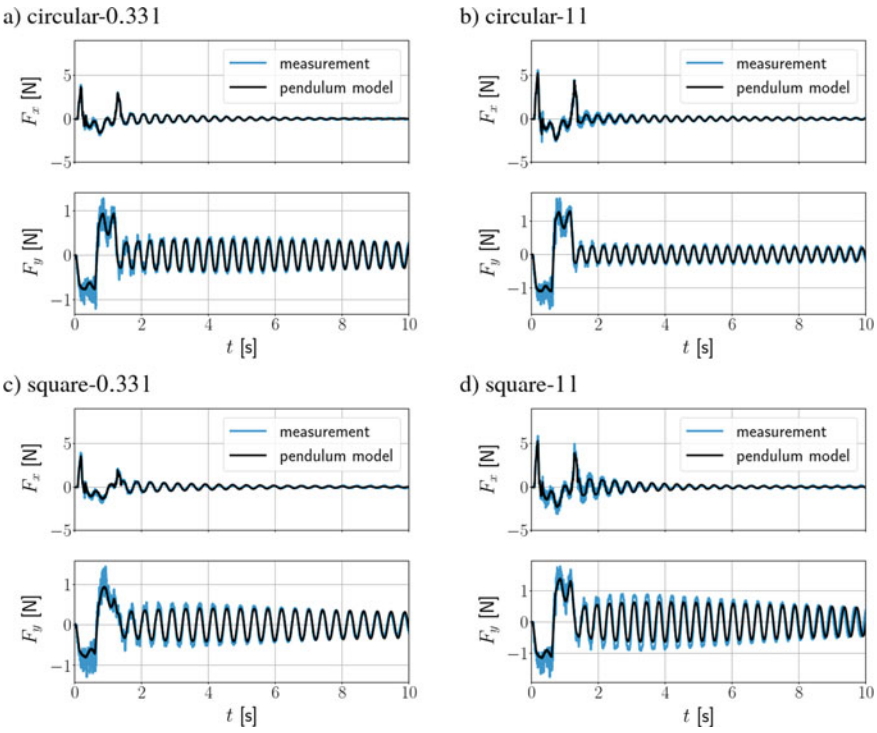

Fig. 19.4 Comparison of measurements and simulations results of the forces based on the semicircular-shaped trajectory with radius 80 mm for different container configurations

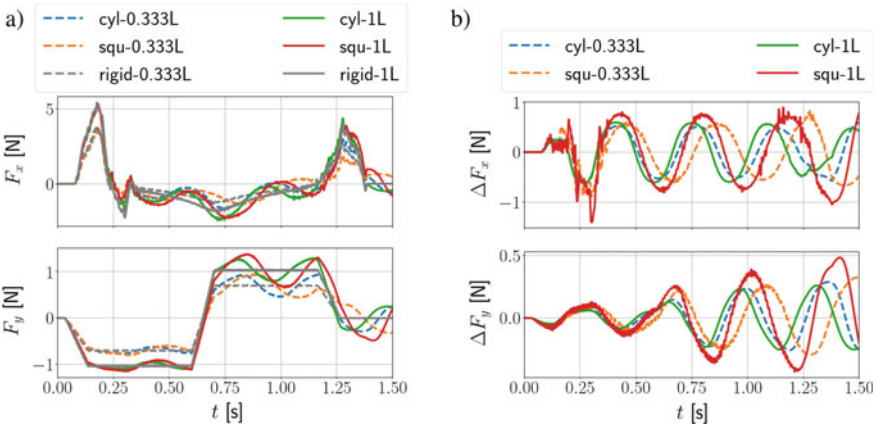

Fig. 19.5 Forces of the semicircular-shaped trajectory with radius 80 mm **a** absolute forces and **b** computed sloshing forces relative to a rigid mass movement

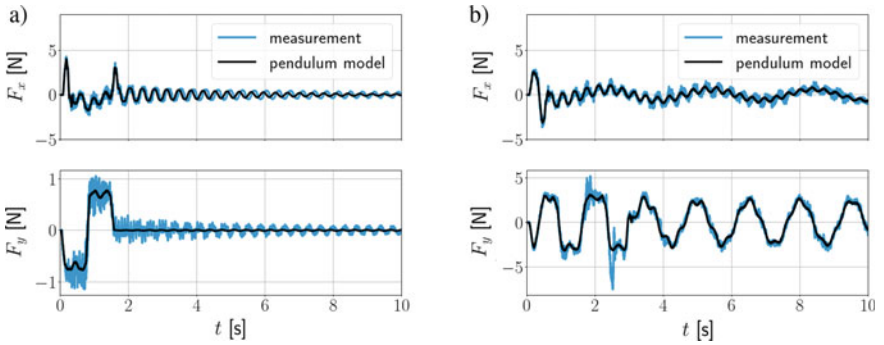

Fig. 19.6 Validation of the forces for the container with circular cross section and 0.33 l filling level for **a** the semicircular-shaped trajectory with radius 130 mm and **b** the eight-shaped trajectory

In addition, Fig. 19.6b shows the results for the same container configuration but for the eight-shaped trajectory. In contrast to all other experiments, here the liquid-filled container is in continuous motion. Also in this case, excellent agreement between measurement and simulation results can be observed. This leads to the conclusion that the pendulum model with identified parameters is sufficient accurate and robust for the representation of sloshing in moving liquid-filled containers.

19.5 Smoothed Particle Hydrodynamics Simulations

In addition to the experimental measurements, sloshing in moving containers is numerically investigated using the SPH method, which employs discrete Lagrangian mass elements (so-called fluid particles) instead of a mesh-based spatial discretization. For free-surface flow phenomena, this meshless nature is of specific advantage, since the Lagrangian fluid particles inherently allow the representation of the dynamic liquid surface, without any additional modeling complications, such as typically required for mesh-based methods.

The simulations are conducted using the particle simulation software LIGGGHTS [3], coupled to the mechatronic systems simulation package HOTINT [4, 5]. This coupling facilitates SPH simulations in the context of fluid structure interaction (FSI) problems [6]. The SPH model included in LIGGGHTS is based on the classical, weakly compressible formulation as originally introduced by Monaghan [7], and additionally the following specific variants or modifications are used:

- Morris model for viscous forces [8],
- discretized continuity equation for the density [7],
- first-order consistent density filtering by moving least squares (MLS) [9],
- equation of state for liquids according to [7],
- Wendland smoothing kernel [10] and

- explicit time integration by a 2nd order Verlet scheme, see, e.g., [11].

The solid wall boundary conditions are imposed by using the particle-wall interaction model according to [12]. Moreover, another correction is employed to the density field in order to avoid the accumulation of errors due to the numerical time integration of the continuity equation, which may lead to inconsistencies between mass, density, and volume. More details about this correction and the used SPH model are provided in previous work [13].

In the SPH simulations, the spatial resolution is varied by using values of 2 and 4 mm for the initial particle spacing, yielding a total particle number of 125000 and 15625 for 1 l of water, respectively. The smoothing length is set to the 1.25-fold of the initial particle spacing in each case, as previous studies [13] revealed to be reasonable. The speed of sound is chosen to be $10\frac{\mathrm{m}}{\mathrm{s}}$, which is sufficient to keep the numerical compressibility negligible under the investigated conditions. With that, a time step of $1e^{-5}$ s is sufficient for numerical stability in most cases, except for the cases with 125000 particles, here the time step is $5e^{-6}$ s. The MLS filter is periodically applied every 10 time steps.

Simulations are conducted for the same scenarios as in Sect. 19.4. The resulting forces in the x- and y-direction over time are shown in Fig. 19.7 compared to the corresponding measurement data. For the semicircular-shaped trajectory, excellent agreement of the forces is achieved during the movement (until approx. 1.4 s). In some cases the post-excitation sloshing agrees well too, specifically $F_x(t)$ for the cases with 0.33 l. Generally, $F_y(t)$ shows less agreement than the $F_x(t)$ and the cases with 0.33 l show better agreement than the cases with 1 l. However, the sloshing frequency agrees well in all cases, and the damping rate is similar between measurements and SPH results with 2 mm particle spacing. The 4 mm SPH results show significantly higher damping, therefore, the post-excitation sloshing is distinctly better reproduced by the 2 mm SPH resolution. Clearly, the computational expense is usually about the 10-fold with 2 mm compared to 4 mm SPH resolution, and if only the excitation period is of interest, the 4 mm resolution is sufficient (as often the case in automation and control applications).

For the eight-shaped trajectory, the comparison is similar, see Fig. 19.7e. In the first second of the movement, the agreement of the forces obtained from SPH simulations and measurements is excellent. In contrast to the semicircular-shaped trajectory, there is no post-excitation period, since the container is continuously moved along the closed eight-shaped trajectory. Instead of that, there are higher sloshing modes superposed, whose amplitudes decrease slowly over time. Interestingly, this is more pronounced in the x-direction, whereas for the semicircular-shaped cases discussed above the post-excitation sloshing amplitude is higher in the y-direction.

In summary, the comparison of the forces from SPH simulations and measurements shows excellent agreement, specifically during the movements. Some differences appear in the post-excitation sloshing. These could be related to the finite stiffness of the experimental setup, which introduces additional dynamics depending on direction and filling level, as well as numerical dissipation in the SPH simulations, which causes additional damping depending on the numerical resolution. Analogous

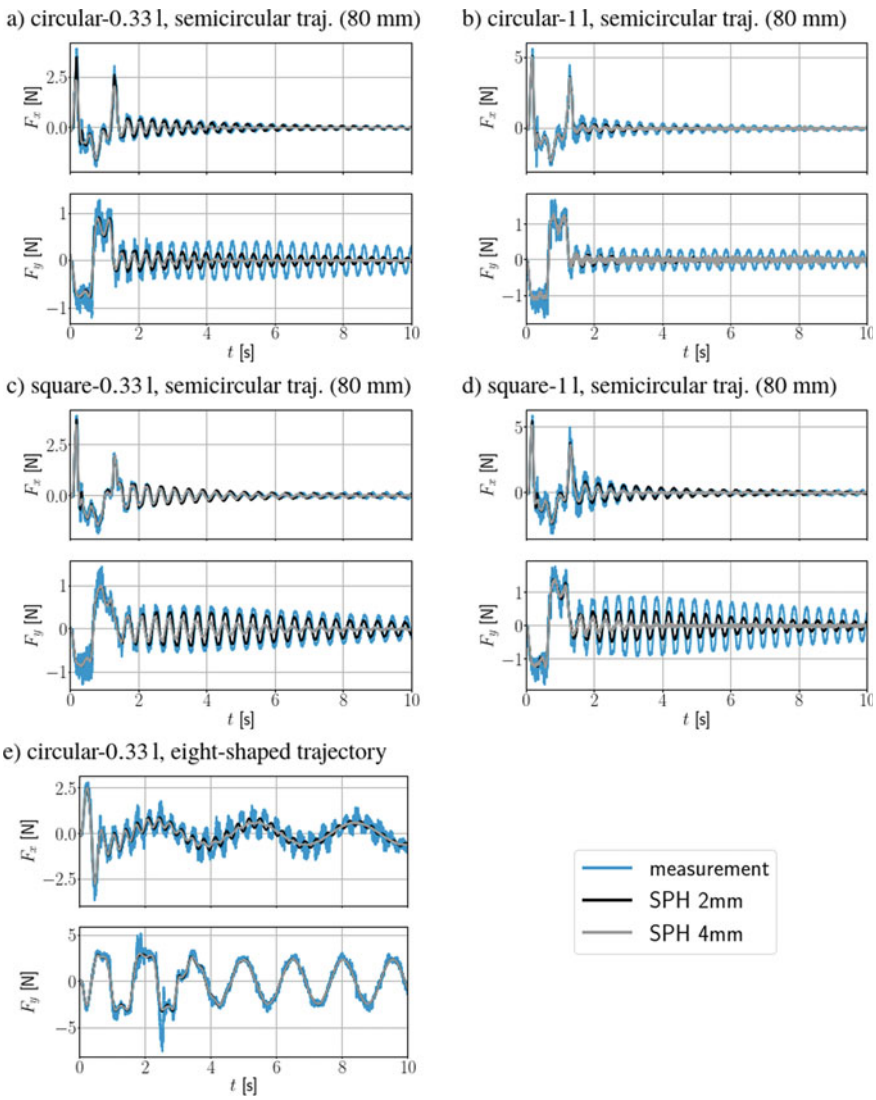

Fig. 19.7 Comparison of forces obtained from SPH simulations and measurements

to the measurements, the SPH results can be used for the parameter identification of the simplified model, which will be discussed in the following section.

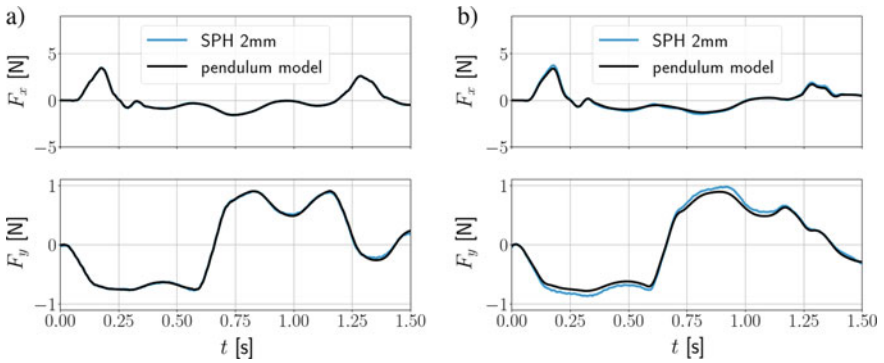

Fig. 19.8 Comparison of SPH and pendulum model simulation results for the semicircular-shaped trajectory with radius 80 mm, filling level 0.33 l, and containers of **a** circular and **b** square cross section

19.6 Parameter Identification Based on the SPH Simulations

Similar to Sect. 19.4, the parameter identification for the pendulum model is repeated based on the SPH simulation results presented in the previous section. In contrast to Sect. 19.5, here only the moving phase of the container is considered for the identification, due to the above-discussed differences during the post-excitation evolution. However, this represents no restriction here, since the focus of this contribution is on the sloshing behavior during the movement in order to address, e.g., optimal trajectory planning of a transportation shuttle, where the evolution of post-excitation effects are of minor interest.

As shown in Fig. 19.8, simulation results of the identified pendulum model for containers with circular and square cross sections and filling level 0.33 l are in excellent agreement with the SPH simulations. Table 19.1 shows a comparison of the parameters identified from SPH results, with the parameters identified from measurement data. Obviously, the pendulum length l agrees well in all cases, while the sloshing mass m shows some deviations, specifically for the container with the square-shaped cross section (18.2%). The damping parameters identified from SPH results differ strongly, which results from the exclusion of the post-excitation phase in that case.

Table 19.1 Comparison of the values for the identified pendulum parameters with values from the literature [1]

	Circular			Circular			Square			Square		
	0.331			11			0.331			11		
	lit	meas	SPH	lit	meas	SPH	lit	meas	SPH	lit	meas	SPH
m	0.163	0.1630	0.1490	0.178	0.1730	0.1580	0.201	0.1980	0.1630	0.256	0.2480	0.2030
l	0.030	0.0309	0.0305	0.027	0.0280	0.0279	0.041	0.0415	0.0407	0.032	0.0338	0.0342
d_{px}		0.097	0.110		0.062	0.200		0.088	0.019		0.156	0.091
d_{py}		0.016	0.000		0.020	0.000		0.025	0.000		0.037	0.000

19.7 Conclusion

Liquid sloshing in containers of different geometries that are transported along different trajectories is investigated by considering the forces acting on the container. Comparisons with measurements show that the system dynamics can be accurately reproduced by a pendulum model. Simulations based on smoothed particle hydrodynamics (SPH) provide results in excellent agreement to the measurements too. However, special attention must be paid to the damping behavior. These investigations justify the approach of identifying the pendulum model parameters based on SPH simulation results.

As a final result, it can be shown that this approach yields reliable values for the main model parameters, such that it is reasonable to replace experiments with simulations in this context in order to reduce costs and time. Future activities will take advantage of the simple pendulum model for trajectory planning and optimization for fast container transport to prevent the liquid from spilling over the container opening by assuring limits of the maximum sloshing angle.

Acknowledgements This work has been supported by the LCM–K2 Center within the framework of the Austrian COMET-K2 program.

References

1. Dodge, F.T.: The new "dynamic behavior of liquids in moving containers". Southwest Research Institute, San Antonio (2000)
2. SyMSpace, Linz Center of Mechatronics GmbH (2020). http://www.lcm.at
3. LIGGGHTS(R): Open source particle simulation code (2020). https://www.cfdem.com
4. Gerstmayr, J., et al.: Hotint: a script language based framework for the simulation of multibody dynamics systems. In: Proceedings of the ASME 2013 IDETC-CIE Conference (2013)
5. HOTINT: A flexible multibody system dyn. freeware code (2020). https://hotint.lcm.at
6. Schörgenhumer, M.: Smoothed particle hydrodynamics with consistent boundaries for fluid-structure interaction, No. 33 in Schriftenreihe Advances in Mechatronics. Trauner Verlag, Linz, Austria (2016)
7. Monaghan, J.J.: Simulating free surface flows with SPH. J. Comput. Phys. **110**(2), 399–406 (1994)

8. Morris, J.P., et al.: Modeling low Reynolds number incompressible flows using SPH. J. Comput. Phys. **136**(1), 214–226 (1997)
9. Gomez-Gesteira, M., et al.: State-of-the-art of classical SPH for free-surface flows. J. Hydraul. Res. **48**(S1), 6–27 (2010)
10. Wendland, H.: Piecewise polynomial, positive definite and compactly supported radial functions of minimal degree. Adv. Comput. Math. **4**, 389–396 (1995)
11. Monaghan, J.J.: Smoothed particle hydrodynamics. Rep. Prog. Phys. **68**(8), 1703–1759 (2005)
12. Eitzlmayr, A., et al.: A novel method for modeling of complex wall geometries in smoothed particle hydrodynamics. Comput. Phys. Commun. **185**(10), 2436–2448 (2014)
13. Schörgenhumer, M., Eitzlmayr, A.: Modeling of liquid sloshing with application in robotics and automation. IFAC-PapersOnLine **52**(15), 253–258 (2019)